

Measurement of CP -violating parameters in fully reconstructed $B \rightarrow D^{(*)\pm} \pi^\mp$ and $B \rightarrow D^\pm \rho^\mp$ decays

The *BABAR* Collaboration

March 10, 2017

Abstract

We present a preliminary measurement of the CP -violating parameters in fully reconstructed $B^0 \rightarrow D^{(*)\pm} \pi^\mp$ and $B^0 \rightarrow D^\pm \rho^\mp$ decays in approximately 232 million $\Upsilon(4S) \rightarrow B\bar{B}$ decays collected with the *BABAR* detector at the PEP-II asymmetric-energy B factory at SLAC. From a maximum likelihood fit to the time-dependent decay distributions we obtain for the parameters related to the CP violation quantity $\sin(2\beta + \gamma)$:

$$\begin{aligned} a^{D\pi} &= -0.013 \pm 0.022 \text{ (stat.)} \pm 0.007 \text{ (syst.)}, & c_{lep}^{D\pi} &= -0.043 \pm 0.042 \text{ (stat.)} \pm 0.011 \text{ (syst.)}, \\ a^{D^*\pi} &= -0.043 \pm 0.023 \text{ (stat.)} \pm 0.010 \text{ (syst.)}, & c_{lep}^{D^*\pi} &= 0.047 \pm 0.042 \text{ (stat.)} \pm 0.015 \text{ (syst.)}, \\ a^{D\rho} &= -0.024 \pm 0.031 \text{ (stat.)} \pm 0.010 \text{ (syst.)}, & c_{lep}^{D\rho} &= -0.098 \pm 0.055 \text{ (stat.)} \pm 0.019 \text{ (syst.)}. \end{aligned}$$

Presented at the International Europhysics Conference On High-Energy Physics (HEP 2005),
7/21—7/27/2005, Lisbon, Portugal

Stanford Linear Accelerator Center, Stanford University, Stanford, CA 94309

Work supported in part by Department of Energy contract DE-AC03-76SF00515.

The BABAR Collaboration,

B. Aubert, R. Barate, D. Boutigny, F. Couderc, Y. Karyotakis, J. P. Lees, V. Poireau, V. Tisserand,
A. Zghiche

Laboratoire de Physique des Particules, F-74941 Annecy-le-Vieux, France

E. Grauges

IFAE, Universitat Autònoma de Barcelona, E-08193 Bellaterra, Barcelona, Spain

A. Palano, M. Pappagallo, A. Pompili

Università di Bari, Dipartimento di Fisica and INFN, I-70126 Bari, Italy

J. C. Chen, N. D. Qi, G. Rong, P. Wang, Y. S. Zhu

Institute of High Energy Physics, Beijing 100039, China

G. Eigen, I. Ofte, B. Stugu

University of Bergen, Institute of Physics, N-5007 Bergen, Norway

G. S. Abrams, M. Battaglia, A. B. Breon, D. N. Brown, J. Button-Shafer, R. N. Cahn, E. Charles,
C. T. Day, M. S. Gill, A. V. Gritsan, Y. Groysman, R. G. Jacobsen, R. W. Kadel, J. Kadyk, L. T. Kerth,
Yu. G. Kolomensky, G. Kukartsev, G. Lynch, L. M. Mir, P. J. Oddone, T. J. Orimoto, M. Pripstein,
N. A. Roe, M. T. Ronan, W. A. Wenzel

Lawrence Berkeley National Laboratory and University of California, Berkeley, California 94720, USA

M. Barrett, K. E. Ford, T. J. Harrison, A. J. Hart, C. M. Hawkes, S. E. Morgan, A. T. Watson

University of Birmingham, Birmingham, B15 2TT, United Kingdom

M. Fritsch, K. Goetzen, T. Held, H. Koch, B. Lewandowski, M. Pelizaeus, K. Peters, T. Schroeder,
M. Steinke

Ruhr Universität Bochum, Institut für Experimentalphysik 1, D-44780 Bochum, Germany

J. T. Boyd, J. P. Burke, N. Chevalier, W. N. Cottingham

University of Bristol, Bristol BS8 1TL, United Kingdom

T. Cuhadar-Donszelmann, B. G. Fulsom, C. Hearty, N. S. Knecht, T. S. Mattison, J. A. McKenna

University of British Columbia, Vancouver, British Columbia, Canada V6T 1Z1

A. Khan, P. Kyberd, M. Saleem, L. Teodorescu

Brunel University, Uxbridge, Middlesex UB8 3PH, United Kingdom

A. E. Blinov, V. E. Blinov, A. D. Bukin, V. P. Druzhinin, V. B. Golubev, E. A. Kravchenko,
A. P. Onuchin, S. I. Serebnyakov, Yu. I. Skovpen, E. P. Solodov, A. N. Yushkov

Budker Institute of Nuclear Physics, Novosibirsk 630090, Russia

D. Best, M. Bondioli, M. Bruinsma, M. Chao, S. Curry, I. Eschrich, D. Kirkby, A. J. Lankford, P. Lund,
M. Mandelkern, R. K. Mommsen, W. Roethel, D. P. Stoker

University of California at Irvine, Irvine, California 92697, USA

C. Buchanan, B. L. Hartfiel, A. J. R. Weinstein

University of California at Los Angeles, Los Angeles, California 90024, USA

S. D. Foulkes, J. W. Gary, O. Long, B. C. Shen, K. Wang, L. Zhang
University of California at Riverside, Riverside, California 92521, USA

D. del Re, H. K. Hadavand, E. J. Hill, D. B. MacFarlane, H. P. Paar, S. Rahatlou, V. Sharma
University of California at San Diego, La Jolla, California 92093, USA

J. W. Berryhill, C. Campagnari, A. Cunha, B. Dahmes, T. M. Hong, M. A. Mazur, J. D. Richman,
W. Verkerke
University of California at Santa Barbara, Santa Barbara, California 93106, USA

T. W. Beck, A. M. Eisner, C. J. Flacco, C. A. Heusch, J. Kroseberg, W. S. Lockman, G. Nesom, T. Schalk,
B. A. Schumm, A. Seiden, P. Spradlin, D. C. Williams, M. G. Wilson
University of California at Santa Cruz, Institute for Particle Physics, Santa Cruz, California 95064, USA

J. Albert, E. Chen, G. P. Dubois-Felsmann, A. Dvoretzki, D. G. Hitlin, I. Narsky, T. Piatenko,
F. C. Porter, A. Ryd, A. Samuel
California Institute of Technology, Pasadena, California 91125, USA

R. Andreassen, S. Jayatilleke, G. Mancinelli, B. T. Meadows, M. D. Sokoloff
University of Cincinnati, Cincinnati, Ohio 45221, USA

F. Blanc, P. Bloom, S. Chen, W. T. Ford, J. F. Hirschauer, A. Kreisel, U. Nauenberg, A. Olivas,
P. Rankin, W. O. Ruddick, J. G. Smith, K. A. Ulmer, S. R. Wagner, J. Zhang
University of Colorado, Boulder, Colorado 80309, USA

A. Chen, E. A. Eckhart, J. L. Harton, A. Soffer, W. H. Toki, R. J. Wilson, Q. Zeng
Colorado State University, Fort Collins, Colorado 80523, USA

D. Altenburg, E. Feltresi, A. Hauke, B. Spaan
Universität Dortmund, Institut für Physik, D-44221 Dortmund, Germany

T. Brandt, J. Brose, M. Dickopp, V. Klose, H. M. Lacker, R. Nogowski, S. Otto, A. Petzold, G. Schott,
J. Schubert, K. R. Schubert, R. Schwierz, J. E. Sundermann
Technische Universität Dresden, Institut für Kern- und Teilchenphysik, D-01062 Dresden, Germany

D. Bernard, G. R. Bonneaud, P. Grenier, S. Schrenk, Ch. Thiebaux, G. Vasileiadis, M. Verderi
Ecole Polytechnique, LLR, F-91128 Palaiseau, France

D. J. Bard, P. J. Clark, W. Gradl, F. Muheim, S. Playfer, Y. Xie
University of Edinburgh, Edinburgh EH9 3JZ, United Kingdom

M. Andreotti, V. Azzolini, D. Bettoni, C. Bozzi, R. Calabrese, G. Cibinetto, E. Luppi, M. Negrini,
L. Piemontese
Università di Ferrara, Dipartimento di Fisica and INFN, I-44100 Ferrara, Italy

F. Anulli, R. Baldini-Ferrolì, A. Calcaterra, R. de Sangro, G. Finocchiaro, P. Patteri, I. M. Peruzzi,¹
M. Piccolo, A. Zallo
Laboratori Nazionali di Frascati dell'INFN, I-00044 Frascati, Italy

¹Also with Università di Perugia, Dipartimento di Fisica, Perugia, Italy

A. Buzzo, R. Capra, R. Contri, M. Lo Vetere, M. Macri, M. R. Monge, S. Passaggio, C. Patrignani,
E. Robutti, A. Santroni, S. Tosi

Università di Genova, Dipartimento di Fisica and INFN, I-16146 Genova, Italy

G. Brandenburg, K. S. Chaisanguanthum, M. Morii, E. Won, J. Wu

Harvard University, Cambridge, Massachusetts 02138, USA

R. S. Dubitzky, U. Langenegger, J. Marks, S. Schenk, U. Uwer

Universität Heidelberg, Physikalisches Institut, Philosophenweg 12, D-69120 Heidelberg, Germany

W. Bhimji, D. A. Bowerman, P. D. Dauncey, U. Egede, R. L. Flack, J. R. Gaillard, G. W. Morton,
J. A. Nash, M. B. Nikolich, G. P. Taylor, W. P. Vazquez

Imperial College London, London, SW7 2AZ, United Kingdom

M. J. Charles, W. F. Mader, U. Mallik, A. K. Mohapatra

University of Iowa, Iowa City, Iowa 52242, USA

J. Cochran, H. B. Crawley, V. Eyges, W. T. Meyer, S. Prell, E. I. Rosenberg, A. E. Rubin, J. Yi

Iowa State University, Ames, Iowa 50011-3160, USA

N. Arnaud, M. Davier, X. Giroux, G. Grosdidier, A. Höcker, F. Le Diberder, V. Lepeltier, A. M. Lutz,
A. Oyanguren, T. C. Petersen, M. Pierini, S. Plaszczynski, S. Rodier, P. Roudeau, M. H. Schune,
A. Stocchi, G. Wormser

Laboratoire de l'Accélérateur Linéaire, F-91898 Orsay, France

C. H. Cheng, D. J. Lange, M. C. Simani, D. M. Wright

Lawrence Livermore National Laboratory, Livermore, California 94550, USA

A. J. Bevan, C. A. Chavez, I. J. Forster, J. R. Fry, E. Gabathuler, R. Gamet, K. A. George,
D. E. Hutchcroft, R. J. Parry, D. J. Payne, K. C. Schofield, C. Touramanis

University of Liverpool, Liverpool L69 7ZE, United Kingdom

C. M. Cormack, F. Di Lodovico, W. Menges, R. Sacco

Queen Mary, University of London, E1 4NS, United Kingdom

C. L. Brown, G. Cowan, H. U. Flaecher, M. G. Green, D. A. Hopkins, P. S. Jackson, T. R. McMahon,
S. Ricciardi, F. Salvatore

University of London, Royal Holloway and Bedford New College, Egham, Surrey TW20 0EX, United Kingdom

D. Brown, C. L. Davis

University of Louisville, Louisville, Kentucky 40292, USA

J. Allison, N. R. Barlow, R. J. Barlow, C. L. Edgar, M. C. Hodgkinson, M. P. Kelly, G. D. Lafferty,
M. T. Naisbit, J. C. Williams

University of Manchester, Manchester M13 9PL, United Kingdom

C. Chen, W. D. Hulsbergen, A. Jawahery, D. Kovalskyi, C. K. Lae, D. A. Roberts, G. Simi

University of Maryland, College Park, Maryland 20742, USA

G. Blaylock, C. Dallapiccola, S. S. Hertzbach, R. Kofler, V. B. Koptchev, X. Li, T. B. Moore, S. Saremi,
H. Staengle, S. Willocq

University of Massachusetts, Amherst, Massachusetts 01003, USA

R. Cowan, K. Koeneke, G. Sciolla, S. J. Sekula, M. Spitznagel, F. Taylor, R. K. Yamamoto
*Massachusetts Institute of Technology, Laboratory for Nuclear Science, Cambridge, Massachusetts 02139,
USA*

H. Kim, P. M. Patel, S. H. Robertson
McGill University, Montréal, Quebec, Canada H3A 2T8

A. Lazzaro, V. Lombardo, F. Palombo
Università di Milano, Dipartimento di Fisica and INFN, I-20133 Milano, Italy

J. M. Bauer, L. Cremaldi, V. Eschenburg, R. Godang, R. Kroeger, J. Reidy, D. A. Sanders, D. J. Summers,
H. W. Zhao

University of Mississippi, University, Mississippi 38677, USA

S. Brunet, D. Côté, P. Taras, B. Viaud
Université de Montréal, Laboratoire René J. A. Lévesque, Montréal, Quebec, Canada H3C 3J7

H. Nicholson
Mount Holyoke College, South Hadley, Massachusetts 01075, USA

N. Cavallo,² G. De Nardo, F. Fabozzi,² C. Gatto, L. Lista, D. Monorchio, P. Paolucci, D. Piccolo,
C. Sciacca

Università di Napoli Federico II, Dipartimento di Scienze Fisiche and INFN, I-80126, Napoli, Italy

M. Baak, H. Bulten, G. Raven, H. L. Snoek, L. Wilden
*NIKHEF, National Institute for Nuclear Physics and High Energy Physics, NL-1009 DB Amsterdam, The
Netherlands*

C. P. Jessop, J. M. LoSecco
University of Notre Dame, Notre Dame, Indiana 46556, USA

T. Allmendinger, G. Benelli, K. K. Gan, K. Honscheid, D. Hufnagel, P. D. Jackson, H. Kagan, R. Kass,
T. Pulliam, A. M. Rahimi, R. Ter-Antonyan, Q. K. Wong

Ohio State University, Columbus, Ohio 43210, USA

J. Brau, R. Frey, O. Igonkina, M. Lu, C. T. Potter, N. B. Sinev, D. Strom, J. Strube, E. Torrence
University of Oregon, Eugene, Oregon 97403, USA

F. Galeazzi, M. Margoni, M. Morandin, M. Posocco, M. Rotondo, F. Simonetto, R. Stroili, C. Voci
Università di Padova, Dipartimento di Fisica and INFN, I-35131 Padova, Italy

M. Benayoun, H. Briand, J. Chauveau, P. David, L. Del Buono, Ch. de la Vaissière, O. Hamon,
M. J. J. John, Ph. Leruste, J. Malclès, J. Ocariz, L. Roos, G. Therin
*Universités Paris VI et VII, Laboratoire de Physique Nucléaire et de Hautes Energies, F-75252 Paris,
France*

²Also with Università della Basilicata, Potenza, Italy

P. K. Behera, L. Gladney, Q. H. Guo, J. Panetta
University of Pennsylvania, Philadelphia, Pennsylvania 19104, USA

M. Biasini, R. Covarelli, S. Pacetti, M. Pioppi
Università di Perugia, Dipartimento di Fisica and INFN, I-06100 Perugia, Italy

C. Angelini, G. Batignani, S. Bettarini, F. Bucci, G. Calderini, M. Carpinelli, R. Cenci, F. Forti,
M. A. Giorgi, A. Lusiani, G. Marchiori, M. Morganti, N. Neri, E. Paoloni, M. Rama, G. Rizzo, J. Walsh
Università di Pisa, Dipartimento di Fisica, Scuola Normale Superiore and INFN, I-56127 Pisa, Italy

M. Haire, D. Judd, D. E. Wagoner
Prairie View A&M University, Prairie View, Texas 77446, USA

J. Biesiada, N. Danielson, P. Elmer, Y. P. Lau, C. Lu, J. Olsen, A. J. S. Smith, A. V. Telnov
Princeton University, Princeton, New Jersey 08544, USA

F. Bellini, G. Cavoto, A. D'Orazio, E. Di Marco, R. Faccini, F. Ferrarotto, F. Ferroni, M. Gaspero, L. Li
Gioi, M. A. Mazzoni, S. Morganti, G. Piredda, F. Polci, F. Safai Tehrani, C. Voena
Università di Roma La Sapienza, Dipartimento di Fisica and INFN, I-00185 Roma, Italy

H. Schröder, G. Wagner, R. Waldi
Universität Rostock, D-18051 Rostock, Germany

T. Adye, N. De Groot, B. Franek, G. P. Gopal, E. O. Olaiya, F. F. Wilson
Rutherford Appleton Laboratory, Chilton, Didcot, Oxon, OX11 0QX, United Kingdom

R. Aleksan, S. Emery, A. Gaidot, S. F. Ganzhur, P.-F. Giraud, G. Graziani, G. Hamel de Monchenault,
W. Kozanecki, M. Legendre, G. W. London, B. Mayer, G. Vasseur, Ch. Yèche, M. Zito
DSM/Dapnia, CEA/Saclay, F-91191 Gif-sur-Yvette, France

M. V. Purohit, A. W. Weidemann, J. R. Wilson, F. X. Yumiceva
University of South Carolina, Columbia, South Carolina 29208, USA

T. Abe, M. T. Allen, D. Aston, N. van Bakel, R. Bartoldus, N. Berger, A. M. Boyarski, O. L. Buchmueller,
R. Claus, J. P. Coleman, M. R. Convery, M. Cristinziani, J. C. Dingfelder, D. Dong, J. Dorfan, D. Dujmic,
W. Dunwoodie, S. Fan, R. C. Field, T. Glanzman, S. J. Gowdy, T. Hadig, V. Halyo, C. Hast, T. Hryn'ova,
W. R. Innes, M. H. Kelsey, P. Kim, M. L. Kocian, D. W. G. S. Leith, J. Libby, S. Luitz, V. Luth,
H. L. Lynch, H. Marsiske, R. Messner, D. R. Muller, C. P. O'Grady, V. E. Ozcan, A. Perazzo, M. Perl,
B. N. Ratcliff, A. Roodman, A. A. Salnikov, R. H. Schindler, J. Schwiening, A. Snyder, J. Stelzer, D. Su,
M. K. Sullivan, K. Suzuki, S. Swain, J. M. Thompson, J. Va'vra, M. Weaver, W. J. Wisniewski,
M. Wittgen, D. H. Wright, A. K. Yarritu, K. Yi, C. C. Young
Stanford Linear Accelerator Center, Stanford, California 94309, USA

P. R. Burchat, A. J. Edwards, S. A. Majewski, B. A. Petersen, C. Roat
Stanford University, Stanford, California 94305-4060, USA

M. Ahmed, S. Ahmed, M. S. Alam, J. A. Ernst, M. A. Saeed, F. R. Wappler, S. B. Zain
State University of New York, Albany, New York 12222, USA

W. Bugg, M. Krishnamurthy, S. M. Spanier
University of Tennessee, Knoxville, Tennessee 37996, USA

R. Eckmann, J. L. Ritchie, A. Satpathy, R. F. Schwitters
University of Texas at Austin, Austin, Texas 78712, USA

J. M. Izen, I. Kitayama, X. C. Lou, S. Ye
University of Texas at Dallas, Richardson, Texas 75083, USA

F. Bianchi, M. Bona, F. Gallo, D. Gamba
Università di Torino, Dipartimento di Fisica Sperimentale and INFN, I-10125 Torino, Italy

M. Bomben, L. Bosisio, C. Cartaro, F. Cossutti, G. Della Ricca, S. Dittongo, S. Grancagnolo, L. Lanceri,
L. Vitale
Università di Trieste, Dipartimento di Fisica and INFN, I-34127 Trieste, Italy

F. Martinez-Vidal
IFIC, Universitat de Valencia-CSIC, E-46071 Valencia, Spain

R. S. Panvini³
Vanderbilt University, Nashville, Tennessee 37235, USA

Sw. Banerjee, B. Bhuyan, C. M. Brown, D. Fortin, K. Hamano, R. Kowalewski, J. M. Roney, R. J. Sobie
University of Victoria, Victoria, British Columbia, Canada V8W 3P6

J. J. Back, P. F. Harrison, T. E. Latham, G. B. Mohanty
Department of Physics, University of Warwick, Coventry CV4 7AL, United Kingdom

H. R. Band, X. Chen, B. Cheng, S. Dasu, M. Datta, A. M. Eichenbaum, K. T. Flood, M. Graham,
J. J. Hollar, J. R. Johnson, P. E. Kutter, H. Li, R. Liu, B. Mellado, A. Mihalyi, Y. Pan, R. Prepost,
P. Tan, J. H. von Wimmersperg-Toeller, S. L. Wu, Z. Yu
University of Wisconsin, Madison, Wisconsin 53706, USA

H. Neal
Yale University, New Haven, Connecticut 06511, USA

³Deceased

1 INTRODUCTION

While the measurement of $\sin 2\beta$ is now a precision measurement [1, 2], the constraints on the other two angles of the Unitarity Triangle [3], α and γ , are still limited by statistics and by theoretical uncertainties. We report on the measurement of CP -violating asymmetries in $B^0 \rightarrow D^{(*)\pm} \pi^\mp$ and $B^0 \rightarrow D^\pm \rho^\mp$ decays in $\Upsilon(4S) \rightarrow B\bar{B}$ decays, which are related to $\sin(2\beta + \gamma)$ [4, 5]. This analysis updates results already presented in Ref. [6] using a larger data sample (232 million instead of 110 million $\Upsilon(4S) \rightarrow B\bar{B}$ decays), and complements the recently published *BABAR* measurement of CP violation in $B \rightarrow D^{*\pm} \pi^\mp$ decays with a partial reconstruction technique [7].

The time evolution of $B^0 \rightarrow D^{(*)\pm} h^\mp$ decays, where h^\mp is a charged meson made of u and d quarks, is sensitive to γ because the CKM-favored decay amplitude $\bar{B}^0 \rightarrow D^{(*)+} h^-$, which is proportional to the CKM matrix elements $V_{cb}V_{ud}^*$, and the doubly-CKM-suppressed decay amplitude $B^0 \rightarrow D^{(*)+} h^-$, which is proportional to $V_{cd}V_{ub}^*$, interfere due to $B^0\bar{B}^0$ mixing. The weak phase difference between the two decay amplitudes is γ . When combined with $B^0\bar{B}^0$ mixing, the total weak phase difference between the interfering amplitudes is $2\beta + \gamma$.

The decay rate distribution for $B^0 \rightarrow D^{(*)\pm} h^\mp$ decays, neglecting the decay width difference, is given by

$$f^\pm(\eta, \Delta t) = \frac{e^{-|\Delta t|/\tau}}{4\tau} \times [1 \mp S_\zeta \sin(\Delta m_d \Delta t) \mp \eta C \cos(\Delta m_d \Delta t)], \quad (1)$$

where τ is the B^0 lifetime, Δm_d is the $B^0\bar{B}^0$ mixing frequency, and $\Delta t = t_{\text{rec}} - t_{\text{tag}}$ is the time of the $B^0 \rightarrow D^{(*)\pm} h^\mp$ decay (B_{rec}) relative to the decay of the other B (B_{tag}). In this equation the upper (lower) sign refers to the flavor of B_{tag} as B^0 (\bar{B}^0), while $\eta = +1$ (-1) and $\zeta = +$ ($-$) for the final state $D^{(*)-} h^+$ ($D^{(*)+} h^-$). In the Standard Model, the S and C parameters can be expressed as

$$S_\pm = -\frac{2\text{Im}(\lambda_\pm)}{1 + |\lambda_\pm|^2}, \quad \text{and} \quad C = \frac{1 - r^2}{1 + r^2}, \quad (2)$$

where $r \equiv |\lambda_+| = 1/|\lambda_-|$ and

$$\lambda_\pm = \frac{q}{p} \frac{A(\bar{B}^0 \rightarrow D^\mp h^\pm)}{A(B^0 \rightarrow D^\mp h^\pm)} = r^{\pm 1} e^{-i(2\beta + \gamma \mp \delta)}. \quad (3)$$

Here $\frac{q}{p}$ is a function of the elements of the mixing Hamiltonian [8], and δ is the relative strong phase between the two contributing amplitudes. In these equations, the parameters r and δ depend on the choice of the final state and will be indicated as $r^{D\pi}$, $\delta^{D\pi}$, in the $B^0 \rightarrow D^\pm \pi^\mp$ case, and $r^{D\rho}$, $\delta^{D\rho}$, in the $B^0 \rightarrow D^\pm \rho^\mp$ case. For the $B^0 \rightarrow D^{*\pm} \pi^\mp$ mode the expression is similar with $r^{D^*\pi}$ and $\delta^{D^*\pi}$ (according to Ref. [5] the strong phase is $\delta^{D^*\pi} + \pi$ in this mode, but this does not affect this measurement). Interpreting the S and C parameters in terms of the angles of the Unitarity Triangle requires knowledge of the r parameters. The r parameters are expected to be small (~ 0.02) and therefore cannot be extracted from the measurement of C with the current statistics. They can be estimated, assuming $SU(3)$ symmetry and neglecting contributions from annihilation diagrams, from the ratios of branching fractions $\mathcal{B}(B^0 \rightarrow D_s^{(*)+} \pi^-) / \mathcal{B}(B^0 \rightarrow D^{(*)-} \pi^+)$ and $\mathcal{B}(B^0 \rightarrow D_s^+ \rho^-) / \mathcal{B}(B^0 \rightarrow D^- \rho^+)$ [4, 6, 7]. Note that the $B^0 \rightarrow D_s^{*+} \pi^-$ and $B^0 \rightarrow D_s^+ \rho^-$ decays [9] have not yet been observed.

2 THE BABAR DETECTOR AND DATASET

This measurement is based on 232 million $\Upsilon(4S) \rightarrow B\bar{B}$ decays collected with the *BABAR* detector at the PEP-II storage ring. The *BABAR* detector is described elsewhere [10]. We use Monte Carlo simulation of the *BABAR* detector based on GEANT4 [11] to validate the analysis procedure and to estimate some of the backgrounds.

3 ANALYSIS METHOD

The analysis strategy is similar to our previous publications on this topic [6, 12] and to other time-dependent measurements performed at *BABAR* [1].

We reconstruct the B_{rec} in the $D^\pm\pi^\mp$, $D^{*\pm}\pi^\mp$ and $D^\pm\rho^\mp$ final states. Candidate $B \rightarrow D^{*\pm}\pi^\mp$ decays are reconstructed with the $D^{*\pm}$ decaying to $\bar{D}^0\pi^\pm$, where the \bar{D}^0 subsequently decays to one of the four modes $K^\mp\pi^\pm$, $K^\mp\pi^\pm\pi^0$, $K^\mp\pi^\pm\pi^\mp\pi^\pm$, or $K_S^0\pi^\pm\pi^\mp$. Candidate $B \rightarrow D^\pm\pi^\mp$ and $B \rightarrow D^\pm\rho^\mp$ decays are reconstructed with the D^\pm decaying into $K^\mp\pi^\pm\pi^\pm$ and $K_S^0\pi^\pm$, and the ρ^\pm decaying into $\pi^\pm\pi^0$. The $D^{(*)\pm}$ candidates are then combined with either a single track or a track and a π^0 candidate with invariant mass in the ρ^\pm window, $620 < m(\pi^\pm\pi^0) < 920$ MeV/ c^2 . Exploiting the spin properties of the decay of a pseudo-scalar meson into a pseudo-scalar and a vector meson, we require the cosine of the helicity angle θ_{hel} , defined as the angle between the charged pion and the D momentum in the ρ^\pm rest frame, to satisfy $|\cos\theta_{\text{hel}}| > 0.4$. No requirement is applied on any helicity angle of the $B \rightarrow D^{*\pm}\pi^\mp$ decay channel. The event selection and candidate reconstruction are described in more details in Refs. [6, 12].

To identify the flavor of the B_{tag} , we use multivariate algorithms that identify signatures in the B decay products that determine (“tag”) the flavor to be either a B^0 or a \bar{B}^0 . Primary leptons from semi-leptonic B decays are selected from identified electrons and muons and from isolated energetic tracks. The charges of identified kaons and soft pions from D^{*+} decays are also used to extract flavor information. These algorithms are combined, taking into account the correlations among different sources of flavor information, and provide an estimate of the mistag probability. The tagging procedure has been improved with respect to the procedure used in our previous analysis [6] with the addition of information from low momentum electrons, $\Lambda \rightarrow p\pi$ decays, and correlations among identified kaon candidates. Each event with mistag probability less than 45% is assigned to one of six hierarchical, mutually exclusive tagging categories. The lepton tagging category contains events with an identified lepton, while other events are divided into categories based on the mistag probability. The effective efficiency of the tagging algorithm, defined as $Q = \sum_i \epsilon_i (1 - 2w_i)^2$, where ϵ_i and w_i are the efficiency and the mistag probability for the tagging category i , respectively, improves by 5% (relative) over the algorithm used in Ref. [6].

The time difference Δt is calculated from the measured separation along the beam collision axis Δz between the B_{rec} and B_{tag} decay vertices. We determine the B_{rec} vertex from its charged tracks. The B_{tag} decay vertex is obtained by fitting tracks that do not belong to B_{rec} , imposing constraints on the B_{rec} momentum and the beam-spot location. The Δt resolution is approximately 1.1 ps.

Signal and background are discriminated by two kinematic variables: the beam-energy substituted mass, $m_{\text{ES}} \equiv \sqrt{(\sqrt{s}/2)^2 - p_B^{*2}}$, and the difference between the B candidate’s measured energy and the beam energy, $\Delta E \equiv E_B^* - (\sqrt{s}/2)$. E_B^* (p_B^*) is the energy (momentum) of the B candidate in the e^+e^- center-of-mass frame, and \sqrt{s} is the total center-of-mass energy. The signal region is defined to be $|\Delta E| < 3\sigma$, where the resolution σ is mode-dependent and is approximately

20 MeV as determined from data. Figure 1 shows the m_{ES} distribution for candidates in the signal region.

The background remaining after the event selection can be separated into two categories, one of which is due to random combinations of particles in the event (*combinatorial* background) and the other is due to B decays into final states similar to the signal final states, which have an m_{ES} distribution similar to the signal (*peaking* background).

The m_{ES} distribution of signal events is described by a Gaussian having a width of about $2.5 \text{ MeV}/c^2$, whereas the peaking background is described by a bifurcated Gaussian with widths of about $3 \text{ MeV}/c^2$ on the left side and $2.5 \text{ MeV}/c^2$ on the right side. To separate the combinatorial background, the m_{ES} distribution is fitted with the sum of a threshold function [13] and the signal and peaking background components.

We estimate the contributions of background peaking in the m_{ES} signal region using simulated events. The most dominant peaking background modes are B decays into open-charm final states similar to that of the signal, *e.g.* $B^0 \rightarrow D^{*-}K^+$, $B^+ \rightarrow \bar{D}^{*0}\pi^+/\rho^+$ or $B^0 \rightarrow D^{*-}\rho^+$. The Gaussian yields and the amounts of peaking background are summarized in Table 1. The latter are identified by their source as either coming from neutral or charged B meson decays. In the case of the

Table 1: Signal yields, purities P , and fractions of peaking backgrounds f_{peak} of the selected samples for events with tagging information. The purity is computed in the signal region, for m_{ES} in a three σ region around the B^0 mass nominal value.

Decay mode	yields	$P(\%)$	$f_{peak}(\%)$	
			B^0	B^\pm
$B \rightarrow D^\pm \pi^\mp$	15635 ± 135	85.5 ± 0.3	3.3 ± 0.1	1.3 ± 0.1
$B \rightarrow D^{*\pm} \pi^\mp$	14554 ± 126	93.0 ± 0.2	2.8 ± 0.1	0.8 ± 0.1
$B \rightarrow D^\pm \rho^\mp$	8736 ± 105	81.7 ± 0.4	1.3 ± 0.2	1.5 ± 0.2

$B^0 \rightarrow D^\pm \rho^\mp$ decays, an additional source of background must be considered, which has the same final state, $B^0 \rightarrow D^\pm \pi^\mp \pi^0$, where the $\pi^\mp \pi^0$ system is not produced through the ρ resonance. This background can introduce a dependence of the λ parameter of Eq. 3 on the $\pi\pi^0$ invariant mass: its contribution has been studied in Ref. [6]. This part of the analysis is not updated in this paper; we use our old result in the evaluation of the systematic error (section 4).

An unbinned maximum likelihood fit is performed to the time distribution of events in this sample. Taking into account possible CP violation effects on the tag side [14] the likelihood for signal events of Eq. 1 for each tagging category i and for each decay mode $\mu = D^\pm \pi^\mp, D^{*\pm} \pi^\mp, D^\pm \rho^\mp$ becomes:

$$f_i^{\pm,\mu}(\eta, \Delta t) = \frac{e^{-|\Delta t|/\tau}}{4\tau} \times [1 \mp (a^\mu \mp \eta b_i - \eta c_i^\mu) \sin(\Delta m_d \Delta t) \mp \eta \cos(\Delta m_d \Delta t)], \quad (4)$$

where in the Standard Model

$$\begin{aligned} a^\mu &= 2r^\mu \sin(2\beta + \gamma) \cos \delta^\mu, \\ b_i &= 2r'_i \sin(2\beta + \gamma) \cos \delta'_i, \\ c_i^\mu &= 2 \cos(2\beta + \gamma)(r^\mu \sin \delta^\mu - r'_i \sin \delta'_i). \end{aligned} \quad (5)$$

Here r'_i (δ'_i) is, for each tagging category, the effective amplitude (phase) used to parameterize the tag side interference. Terms of order $r^{\mu 2}$ and $r_i'^2$ have been neglected. Results are quoted only

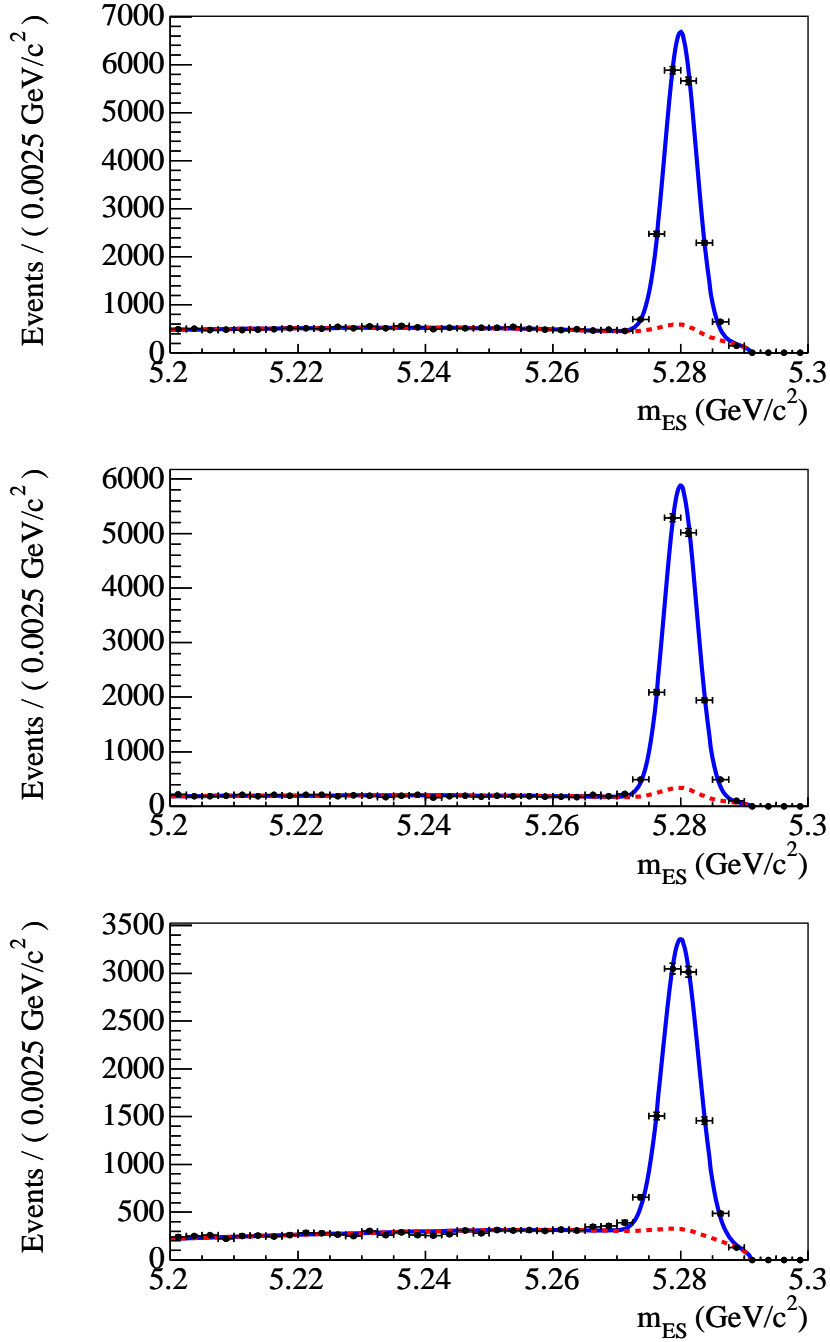


Figure 1: m_{ES} distributions in the signal region for, from top to bottom, the $B \rightarrow D^{\pm}\pi^{\mp}$, $B \rightarrow D^{*\pm}\pi^{\mp}$ and $B \rightarrow D^{\pm}\rho^{\mp}$ sample for events with tagging information. Each solid curve represents the result of a fit with a Gaussian (that describes signal events) plus a bifurcated Gaussian (that describes peaking background events) plus a threshold function (that describes combinatorial background events). Each dashed curve represents the background events only.

for the six a^μ and c_{lep}^μ parameters, which are independent of the unknown parameters r'_i and δ'_i (semi-leptonic B decays have no doubly CKM-suppressed contributions and therefore $r'_{lep} \equiv 0$). The other parameters are constrained by the fit, but, as they depend on r'_i and δ'_i , they do not contribute to the interpretation of the result in terms of $\sin(2\beta + \gamma)$.

The signal Δt distribution in Eq. 4 is convoluted with the resolution function parametrized with the sum of three Gaussians to take into account finite Δt resolution. The probabilities of incorrect tagging (w_i) are accounted for by multiplying the a^μ , c_i^μ parameters and the $\cos(\Delta m_d \Delta t)$ term by the dilutions $D_i = 1 - 2w_i$ (average dilutions for B^0 and \bar{B}^0). Possible differences in mistag probabilities for B^0 and \bar{B}^0 are also taken into account. The resolution function and the tagging parameters are floated in the fit to the data and are consistent within errors with previous *BABAR* analyses [1].

The likelihood function has a contribution for each source of background. The combinatorial background is parametrized as the sum of a component with zero lifetime and one with an effective lifetime floated in the fit to the data. The fraction of each background component is determined from the events in the m_{ES} sidebands, having $5.20 < m_{ES} < 5.27 \text{ GeV}/c^2$. The background events are described using effective dilution parameters, obtained from the fit to the data, and have a Δt resolution function consisting of the sum of two Gaussians, also floated in the fit to the data. The charmed peaking background coming from B^\pm mesons is modeled by an exponential with the B^\pm lifetime, and its amount is fixed to the value predicted by simulation. The resolution function is the same as the signal resolution, while the dilution parameters are fixed to the values obtained from a B^+ control sample. The charmed and charmless peaking backgrounds from B^0 mesons, whose amounts are also fixed to the value estimated from simulation, are modeled with a likelihood similar to the signal likelihood with no CP violation (all the a , b , c parameters fixed to 0). Possible CP violation in this background is taken into account in the evaluation of the systematic uncertainties. The resolution and the dilution parameters are the same as for the signal.

4 SYSTEMATIC STUDIES

Table 2 shows the contributions to the systematic uncertainties of the a and c_{lep} CP parameters.

Table 2: Systematic uncertainties on the a and c parameters.

Source	$B^0 \rightarrow D^\pm \pi^\mp$		$B^0 \rightarrow D^{*\pm} \pi^\mp$		$B^0 \rightarrow D^\pm \rho^\mp$	
	σ_a	σ_c	σ_a	σ_c	σ_a	σ_c
Vertexing ($\sigma_{\Delta t}$)	0.0037	0.0064	0.0080	0.0110	0.0047	0.0110
Fit (σ_{fit})	0.0051	0.0088	0.0052	0.0093	0.0075	0.0129
Model (σ_{mod})	0.0012	0.0013	0.0012	0.0013	0.0001	0.0018
Tagging (σ_{tag})	0.0007	0.0016	0.0011	0.0014	0.0006	0.0012
Background (σ_{bkg})	0.0023	0.0029	0.0020	0.0029	0.0042	0.0070
Dependence on $m_{\pi\pi^0}$ ($\sigma_{\lambda\text{dep}}$)	—	—	—	—	0.0018	0.0047
Total (σ_{tot})	0.0069	0.0114	0.0099	0.0150	0.0100	0.0193

The impact of a possible systematic mis-measurement of Δt ($\sigma_{\Delta t}$) has been estimated by comparing different parameterizations of the resolution function, varying the position of the beam spot, and the absolute z scale within their uncertainties, and loosening and tightening the quality criteria on the reconstructed vertex. We also estimate the impact of the uncertainties on the alignment

of the silicon vertex tracker (SVT) by repeating the measurement using simulated events, intentionally misaligning the SVT in the simulation. As the systematic uncertainty of the fit (σ_{fit}), we quote the upper limit on the bias on the a^μ and c^μ parameters, as estimated from samples of fully-simulated events. The model error (σ_{mod}) contains the uncertainty on the B^0 lifetime and Δm_d , varied by the uncertainties on the world averages [8] and also by floating them in the fit. The tagging error (σ_{tag}) is estimated considering possible differences in tagging efficiency between B^0 and \bar{B}^0 and allowing for different Δt resolutions for correctly and incorrectly tagged events. We also account for uncertainties in the background (σ_{bkg}) by varying the effective lifetimes, dilutions, m_{ES} shape parameters, signal fractions, and background CP asymmetry. For the $B \rightarrow D\rho$ decay we also include the maximum bias of the a and c_{lep} parameters due to the possible dependence of λ on the $\pi\pi^0$ invariant mass ($\sigma_{\lambda\text{dep}}$), as discussed in section 3.

5 PHYSICS RESULTS

From the unbinned maximum likelihood fit we obtain the result:

$$\begin{aligned} a^{D\pi} &= -0.013 \pm 0.022 \text{ (stat.)} \pm 0.007 \text{ (syst.)}, & c_{lep}^{D\pi} &= -0.043 \pm 0.042 \text{ (stat.)} \pm 0.011 \text{ (syst.)}, \\ a^{D^*\pi} &= -0.043 \pm 0.023 \text{ (stat.)} \pm 0.010 \text{ (syst.)}, & c_{lep}^{D^*\pi} &= 0.047 \pm 0.042 \text{ (stat.)} \pm 0.015 \text{ (syst.)}, \\ a^{D\rho} &= -0.024 \pm 0.031 \text{ (stat.)} \pm 0.010 \text{ (syst.)}, & c_{lep}^{D\rho} &= -0.098 \pm 0.055 \text{ (stat.)} \pm 0.019 \text{ (syst.)}. \end{aligned}$$

The largest correlation with any linear combination of other fit parameters is about 20% and 30% for the a^μ and the c_{lep}^μ parameters respectively. Figures 2 to 4 show the Δt distribution for events tagged with leptons (which have the lowest mistag probability for the $B \rightarrow D^\pm \pi^\mp$, $B \rightarrow D^{*\pm} \pi^\mp$, $B \rightarrow D^\pm \rho^\mp$ modes). We combine our result with the result obtained on partially reconstructed $B \rightarrow D^{*\pm} \pi^\mp$ decays [7] and we use the frequentistic method described in Ref. [7] to set a constraint on $|\sin(2\beta + \gamma)|$. The confidence level as a function of $|\sin(2\beta + \gamma)|$ is shown in Fig. 5. We set the lower limits $|\sin(2\beta + \gamma)| > 0.64$ (0.42) @ 68% (90%) confidence level.

6 SUMMARY

We have studied the time evolution of fully reconstructed $B^0 \rightarrow D^{(*)\pm} \pi^\mp$ and $B^0 \rightarrow D^\pm \rho^\mp$ decays in a data sample of 232 million $\Upsilon(4S) \rightarrow B\bar{B}$ decays. CP violation arising from the interference of the CKM-suppressed and the CKM-favored amplitudes is expected to be small but sensitive to $\sin(2\beta + \gamma)$.

The measured CP -violating parameters defined in Eq. 5 are shown in Section 5. No significant CP asymmetry is observed thus far. Using a frequentistic approach and combining our result with the *BABAR* result of Ref. [7], we set the limits: $|\sin(2\beta + \gamma)| > 0.64$ (0.42) @ 68% (90%) confidence level.

7 ACKNOWLEDGMENTS

We are grateful for the extraordinary contributions of our PEP-II colleagues in achieving the excellent luminosity and machine conditions that have made this work possible. The success of this project also relies critically on the expertise and dedication of the computing organizations that support *BABAR*. The collaborating institutions wish to thank SLAC for its support and the

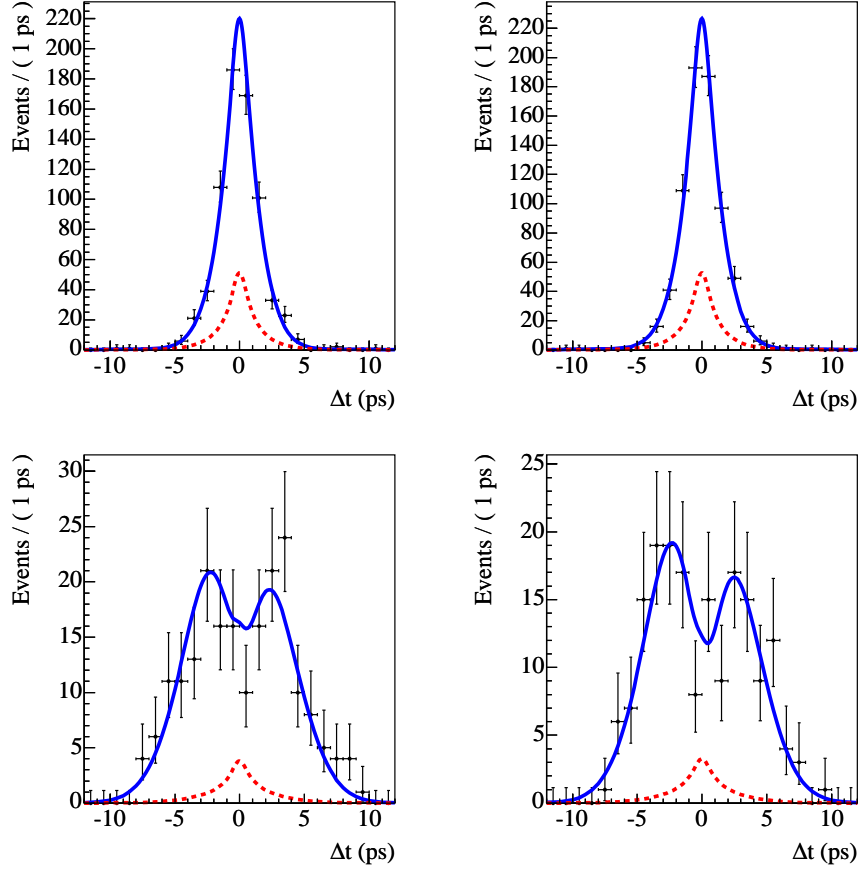


Figure 2: Δt distribution for data having the decay mode $B^0 \rightarrow D^-\pi^+$ in the lepton tagging category for, from upper left going clockwise, $B_{tag} = \bar{B}^0$ and $B_{rec} = D^-\pi^+$, $B_{tag} = B^0$ and $B_{rec} = D^+\pi^-$, $B_{tag} = B^0$ and $B_{rec} = D^-\pi^+$, $B_{tag} = \bar{B}^0$ and $B_{rec} = D^+\pi^-$. The result of the fit is superimposed. In each plot, the dashed curve represents the background contribution.

kind hospitality extended to them. This work is supported by the US Department of Energy and National Science Foundation, the Natural Sciences and Engineering Research Council (Canada), Institute of High Energy Physics (China), the Commissariat à l’Energie Atomique and Institut National de Physique Nucléaire et de Physique des Particules (France), the Bundesministerium für Bildung und Forschung and Deutsche Forschungsgemeinschaft (Germany), the Istituto Nazionale di Fisica Nucleare (Italy), the Foundation for Fundamental Research on Matter (The Netherlands), the Research Council of Norway, the Ministry of Science and Technology of the Russian Federation, and the Particle Physics and Astronomy Research Council (United Kingdom). Individuals have received support from CONACyT (Mexico), the A. P. Sloan Foundation, the Research Corporation, and the Alexander von Humboldt Foundation.

References

- [1] *BABAR* Collaboration, B. Aubert *et al.*, Phys. Rev. Lett. **94**, 161803 (2005).

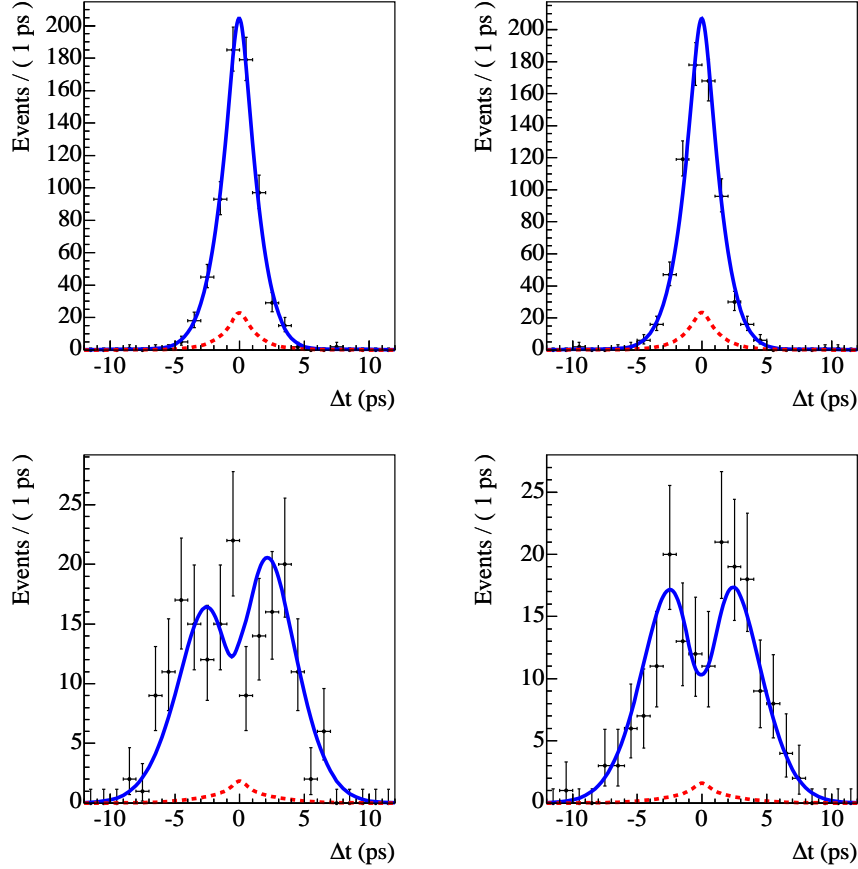


Figure 3: Δt distribution for data having the decay mode $B^0 \rightarrow D^{*-}\pi^+$ in the lepton tagging category for, from upper left going clockwise, $B_{tag} = \bar{B}^0$ and $B_{rec} = D^{*-}\pi^+$, $B_{tag} = B^0$ and $B_{rec} = D^{*+}\pi^-$, $B_{tag} = B^0$ and $B_{rec} = D^{*-}\pi^+$, $B_{tag} = \bar{B}^0$ and $B_{rec} = D^{*+}\pi^-$. The result of the fit is superimposed. In each plot, the dashed curve represents the background contribution.

- [2] Belle Collaboration, K. Abe *et al.*, Phys. Rev. D **71**, 072003 (2005).
- [3] N. Cabibbo, Phys. Rev. Lett. **10**, 531 (1963); M. Kobayashi and T. Maskawa, Prog. Theor. Phys. **49**, 652 (1973).
- [4] I. Dunietz, Phys. Lett. B **427**, 179 (1998); I. Dunietz, R.G. Sachs, Phys. Rev. D **37**, 3186 (1988).
- [5] R. Fleischer, Nucl. Phys. B **671**, 459 (2003).
- [6] BABAR Collaboration, B. Aubert *et al.*, SLAC-PUB-10647, hep-ex/0408038.
- [7] BABAR Collaboration, B. Aubert *et al.*, Phys. Rev. D **71**, 112003 (2005).
- [8] Particle Data Group, S. Eidelman *et al.*, Phys. Lett. B **592**, 1 (2004).
- [9] BABAR Collaboration, B. Aubert *et al.*, SLAC-PUB-10602, hep-ex/0408029.

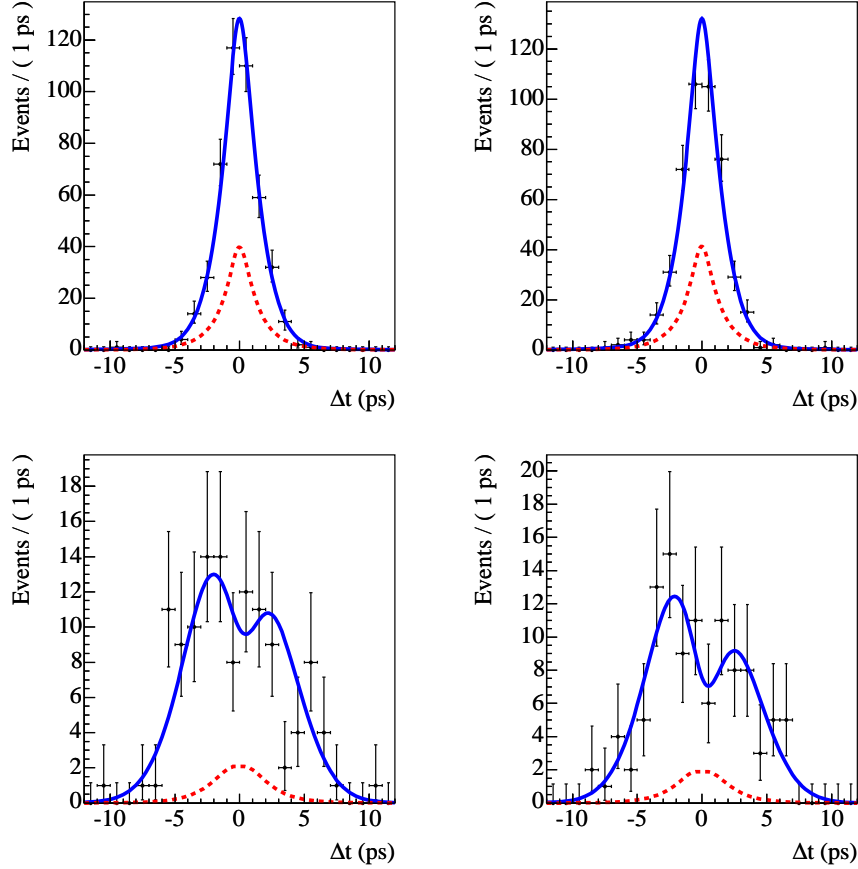


Figure 4: Δt distribution for data having the decay mode $B^0 \rightarrow D^- \rho^+$ in the lepton tagging category for, from upper left going clockwise, $B_{tag} = \bar{B}^0$ and $B_{rec} = D^- \rho^+$, $B_{tag} = B^0$ and $B_{rec} = D^+ \rho^-$, $B_{tag} = B^0$ and $B_{rec} = D^- \rho^+$, \bar{B}^0 and $B_{rec} = D^+ \rho^-$. The result of the fit is superimposed. In each plot, the dashed curve represents the background contribution.

- [10] BABAR Collaboration, B. Aubert *et al.*, Nucl. Instrum. Meth. A **479**, 1 (2002).
- [11] GEANT4 Collaboration, S. Agostinelli *et al.*, Nucl. Instrum. Meth. A **506**, 250 (2003).
- [12] BABAR Collaboration, B. Aubert *et al.*, Phys. Rev. Lett. **92**, 251801 (2004).
- [13] ARGUS Collaboration, H. Albrecht *et al.*, Z. Phys. C **48**, 543 (1990).
- [14] O. Long, M. Baak, R. N. Cahn, and D. Kirkby, Phys. Rev. D **68**, 034010 (2003).

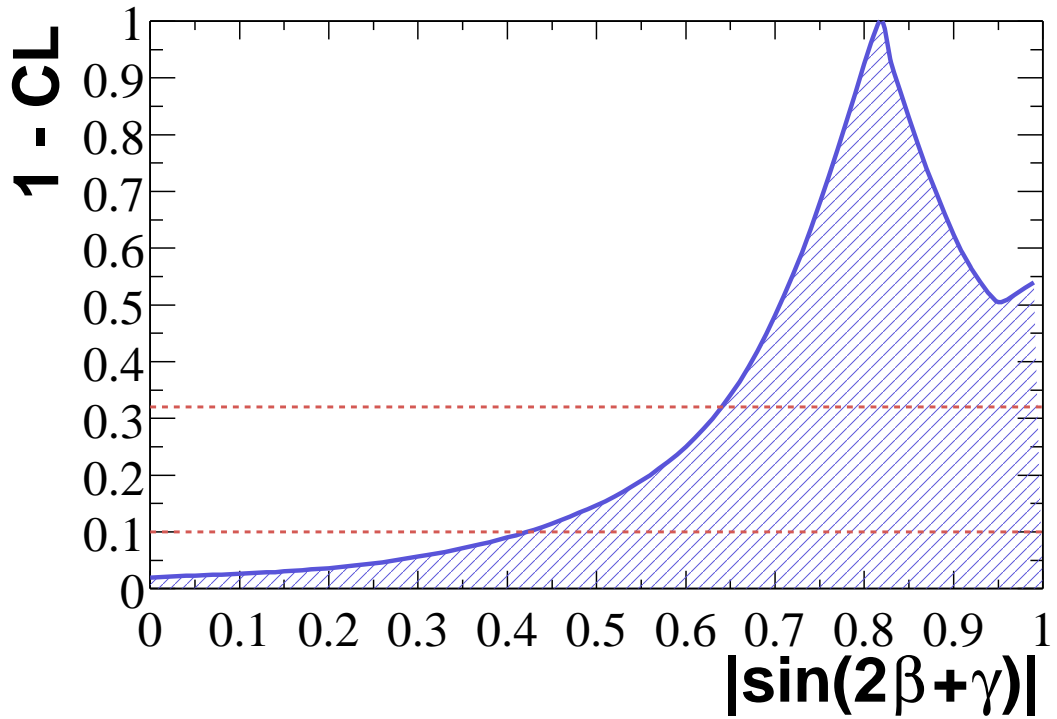


Figure 5: Frequentistic confidence level as a function of $|\sin(2\beta + \gamma)|$, obtained when combining our result with the result previously obtained on partially reconstructed $B \rightarrow D^{*\pm}\pi^\mp$ decays [7]. The horizontal lines show, from top to bottom, the 68% and 90% confidence level.